

## Non-Gaussian velocity distributions in excited granular matter in the absence of clustering

A. Kudrolli\* and J. Henry

*Department of Physics, Clark University, Worcester, Massachusetts 01610*

(Received 18 January 2000)

The velocity distribution of spheres rolling on a slightly tilted rectangular two-dimensional surface is obtained by high speed imaging. The particles are excited by periodic forcing of one of the side walls. Our data suggests that strongly non-Gaussian velocity distributions can occur in dilute granular materials even in the absence of significant density correlations or clustering. When the surface on which the particles roll is tilted further to introduce stronger gravitation, the collision frequency with the driving wall increases and the velocity component distributions approach Gaussian distributions of different widths.

PACS number(s): 81.05.Rm, 05.20.Dd, 45.05.+x

Recent simulations and experiments have shown that clusters are formed due to inelastic collisions in excited granular matter [1–5]. The formation of clusters was shown to lead to non-Gaussian velocity distributions. Here we report that even in the absence of cluster formation or significant density correlations, dissipation leads to strongly non-Gaussian velocity distributions.

The statistical description of dissipative systems such as granular flows are of fundamental interest. Because thermal energies are irrelevant, the concept of “granular temperature” has been introduced based on the velocity fluctuations of particles. A dissipative kinetic theory has been developed to describe rapid granular flows [6]. In this theory, velocity distributions are assumed to be locally Gaussian. Deviations from Maxwell-Boltzmann are explained by averaging over local Gaussian velocity distributions with different widths which are inversely related to the local clustering [7]. Given the success of this local Gaussian distribution assumption, we might conclude that the velocity distributions can be considered to be approximately Gaussian for most practical situations where clustering does not occur. Non-gaussian velocity distributions in the absence of density correlations have been observed in vertically vibrated monolayer which is constrained to nearly two dimensions with a lid [8]. However, the role of particle collisions with the lid on the observed distributions was unclear as vertical velocity was not accessed.

In this Rapid Communication, we study the velocity distributions of steel spheres rolling inside a two-dimensional box for which energy is supplied to the particles by oscillating one of the side walls. A similar system has been used previously to demonstrate the formation of clusters at high densities due to inelastic collisions [4]. However, at low densities corresponding to longer mean free paths and lower collision rates, the particles appear to be randomly distributed and no clustering is observed. We use high speed and high resolution imaging to obtain accurate velocity distributions. Because one of the sides of the rectangular geometry is used to input energy and the particle-particle and particle-wall interactions are dissipative, the velocity distribution is

asymmetrical. An obvious consequence is that the velocity fluctuations in the direction parallel to the driving wall motion is greater than in the perpendicular direction. We find that the velocity distribution is *strongly non-Gaussian even in the direction perpendicular to the motion of the oscillating wall*. By varying the frequency  $f$  and the angle of inclination  $\theta$  of the surface, we show that non-Gaussian velocity distributions can occur when the collision rate due to dissipative interactions is greater than the particle-driving wall collision rate.

The experimental setup consists of one hundred 0.32 cm diameter steel (or brass) spheres rolling on an optically smooth glass surface (29.5 cm  $\times$  24.7 cm) which is enclosed by steel side walls. The setup is similar to that in Ref. [4] with a few enhancements. The coefficient of rolling friction of the spheres on the glass plate is less than  $2 \times 10^{-3}$ . In contrast, the coefficient of sliding friction is  $\sim 0.2$ . The particles are visualized using a SR-1000 Kodak digital camera capable of taking 1000 frames per second (fps). The camera and lights are placed such that the centers of the spheres appear bright. The best pixel resolution of  $512 \times 480$  can be obtained at 250 fps, which was used for most of the data presented here. A typical image is shown in Fig. 1(a). The particles correspond to  $\sim 4$  pixels in diameter and a centroid technique was used to find the position of the particle to within 0.01 cm. The particles with the highest velocities were determined by using images separated by 4 ms, and the velocity of the slowest particles were determined by using images separated by at least 12 ms. The positions of the slow moving particles do not change appreciably in comparison to the pixel size if a very high frame rate is used, resulting in substantial roundoff errors. We note that a combination of both high resolution and high frame rate is required to obtain accurate velocities.

The driving wall is connected to a linear solenoid which is controlled by a computer, and the resulting motion of the piston is measured with a displacement sensor. The displacement of the piston as a function of time,  $d(t)$ , for three typical driving frequencies is plotted in Fig. 1(b). A square waveform of fixed amplitude (4 V) and various frequencies is used to obtain the displacements.

By averaging over at least  $10^5$  images, we obtain velocity distributions of the particles rolling inside the rectangular box. The distributions of the velocity components,  $P(v_x)$

\*Author to whom correspondence should be addressed. Email address: akudrolli@clarku.edu

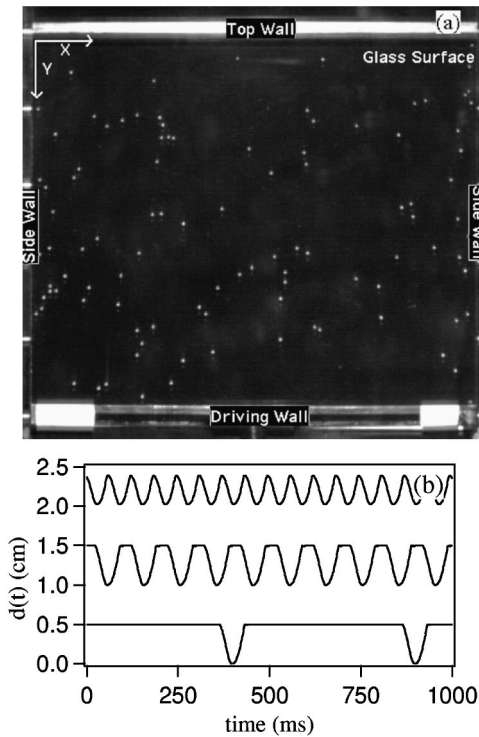


FIG. 1. (a) Image of 100 steel spheres rolling on a glass surface. The surface is tilted at angle  $\theta$  to the horizontal ( $\theta=0.1^\circ$ ). (b) Example of driving wall displacement  $d(t)$  measured using a position sensor for frequencies  $f=2, 10,$  and  $16$  Hz. The displacements for the three cases are offset by 1 cm for clarity. The wall is driven using a linear solenoid.

and  $P(v_y)$ , are plotted in Figs. 2(a) and 2(b), respectively. The directions  $x$  and  $y$  and the origin are indicated in Fig. 1(a). The surface is slightly tilted ( $\theta=0.1^\circ$ ) to continuously excite the particles. Particles that are less than 2 cm from the side walls are excluded to avoid direct effects of the boundaries. We checked that if a narrow region in  $y$  is used, the form of the velocity distributions is independent of  $y$ . The plots in Fig. 2 correspond to various driving frequencies. Note that the form of  $P(v_x)$  and  $P(v_y)$  does not depend strongly on the driving frequency  $f$ . The distribution  $P(v_x)$  is symmetrical about  $v_x=0$ , but is strongly non-Gaussian as can be seen from the poor fit to a Gaussian which is also shown in Fig. 2(a).

The distribution  $P(v_y)$  shown in Fig. 2(b) is non-Gaussian and asymmetrical. The reason for the asymmetry is not difficult to understand. The energy is supplied to the system by the driving wall. Therefore, particles move with higher velocities in the negative- $y$  direction (indicated by the bump at  $v_y \sim -35$  cm/s). The second more subtle reason for the asymmetry is that the particles suffer an inelastic collision either with the wall opposite to the driving wall or with other particles before moving in the positive  $y$  direction. Therefore, particles on average move with lower velocities in the  $+y$  direction than in the  $-y$  direction. Consequently, the particles also spend a longer time interval traveling in the  $+y$  direction than in the  $-y$  direction. Thus, asymmetrical  $v_y$  distributions are obtained by averaging over time. Such effects were also observed in the distributions obtained numerically by Luding *et al.* [9]. The form of  $P(v_x)$  is rela-

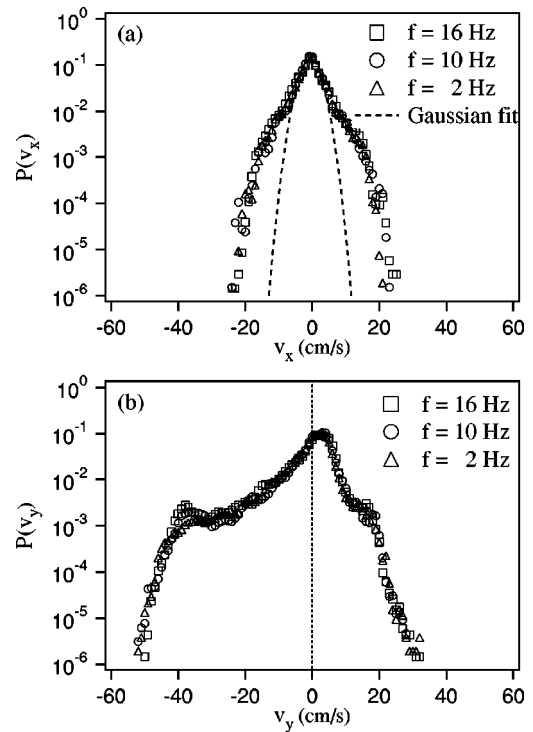


FIG. 2. The probability distribution of velocity components  $v_x$  and  $v_y$  ( $\theta=0.1^\circ$ ). The velocity distributions are strongly non-Gaussian. Note the peak at  $v_y = -35$  cm/s due to the driving wall. The corresponding driving wall displacement  $d(t)$  vs time is shown in Fig. 1(b).

tively independent of the energy input, and therefore its non-Gaussian behavior is surprising.

In Fig. 3(a), we plot  $P(n)$ , the distributions of the number of particles  $n$ , in a  $3 \text{ cm} \times 3 \text{ cm}$  area averaged over the box and over all images. For comparison, the distribution of randomly distributed particles is also shown (dashed curve). This distribution was obtained numerically from an ensemble of 100 particle positions which are separated by at least a particle diameter generated using a random number algorithm. Our data for  $P(n)$  is similar to the randomly distributed case for finite sized particles in a finite container with a small deviation at higher  $n$ . Because of the dilute nature of our experiments (the packing fraction is less than 4%), no effects of clustering are observed as reported in Ref. [4]. In Fig. 3(b), the radial density distribution function  $g(q)$  is plotted as a function the distance normalized by the particle diameter  $q$ .  $g(q)$  does not show oscillations that would indicate clustering and packing. The data does show a slight enhancement at  $q \sim 1$ , but the small deviations are not observed to have significant effect on  $P(v_x)$ , shown in Fig. 2(a).

The effect of gravity and the collision rate with the driving wall is studied by lifting the surface on which the particles roll by the tilt angle  $\theta$ . The  $v_x$  and  $v_y$  distributions are plotted in Fig. 4 corresponding to four values of  $\theta$ . The density distribution  $P(n)$  is no longer uniform in  $y$  as in the  $\theta=0.1^\circ$  case, but decreases strongly with distance from the driving wall. (At the highest angle  $\theta=6.7^\circ$ , the particles do not reach the top wall.) The velocity distributions correspond to particles in a 2 cm wide region at a distance  $y=4$  cm from the driving wall to avoid the effects of the increase in

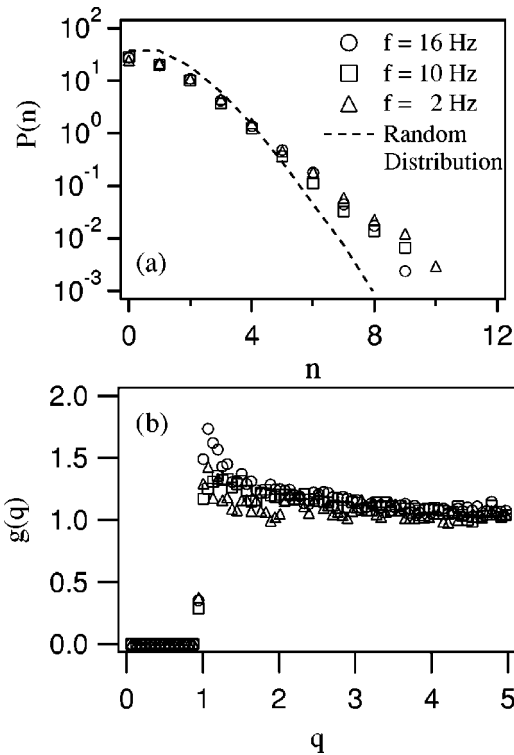


FIG. 3. (a) The distribution of particles  $P(n)$  in a  $3 \text{ cm} \times 3 \text{ cm}$  area. The distribution corresponding to randomly distributed particles is also plotted. (b) The radial correlation function  $g(q)$  as a function of distance normalized by the particle diameter  $q$ . No significant correlation in the distribution is observed.

potential energy and the decrease in the average  $v_y$  at higher  $\theta$ . The distributions  $P(v_x)$  and  $P(v_y)$  grow broader as  $\theta$  increases. A Gaussian fit to the data corresponding to  $\theta = 6.7^\circ$  is shown in Fig. 4. The data for  $P(v_x)$  is reasonably described by a Gaussian especially at low  $v_x$ . However,  $P(v_y)$  deviates systematically from Gaussian because of the asymmetry. Furthermore, the width of  $P(v_y)$  is large compared to the width of  $P(v_x)$  because energy is mostly supplied to the  $x$  component in an inelastic collision, consistent with earlier observations of vertically vibrated granular matter [11]. We further note that  $P(v_x)$  averaged over all  $y$  is non-Gaussian for  $\theta = 6.7^\circ$  because of the slight increase in the widths of the Gaussians as a function of  $y$ . This might also be the reason for deviations from Gaussian observed in velocity distributions of vertically vibrated monolayer layer of particles [12].

As  $\theta$  increases, the acceleration in the  $y$  direction increases. Therefore, the particles fall back to the driving wall faster as  $\theta$  is increased. This results in higher collision rates of particles with the driving wall leading to higher average velocities. Thus, as the collision rate with the driving wall increases, the distributions become broader and more Gaussian. Furthermore, the total number of inelastic collisions the particles undergo before returning to the driving wall decreases because fewer particles hit the top wall at higher  $\theta$ .

We note that there is no discrepancy with the observation of the broadening of the velocity distributions with an increase in  $\theta$  and the data plotted in Fig. 2. It might appear that changing the frequency of the driving piston should also increase the collision rate with the bottom wall and hence have

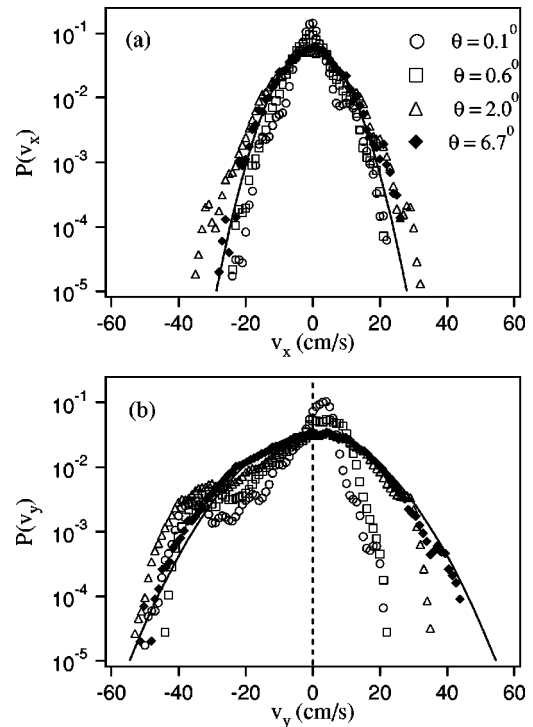


FIG. 4. (a) and (b) Velocity component distributions as a function of inclination angle  $\theta$  ( $f = 10 \text{ Hz}$ ). All particles are in a  $2 \text{ cm}$  wide region at a distance  $y = 16 \text{ cm}$  from the top wall. The  $v_x$  and  $v_y$  distributions approach Gaussians as  $\theta$  is increased. The curves are a Gaussian fit for  $\theta = 6.7^\circ$ .

the same effect. However, the distributions plotted in Fig. 2 do not depend strongly on the driving frequency. The lack of the strong dependence of  $P(v_x)$  and  $P(v_y)$  on  $f$  in Fig. 2 can be explained by the fact that fewer particles are struck by the forward moving wall at higher  $f$ . Thus, the net energy input (and collision rate with the bottom wall) appears to not depend strongly on  $f$ .

Next we discuss the effect of rolling on the distributions. In a previous study, it was noted that rolling appears to lead to a lower effective coefficient of restitution  $r$  during collisions [4]. Some theoretical work has been done studying rolling and collisions [10]. In Fig. 5(a), we plot the  $r$  as a function of scattering angle  $\phi$  of a rolling steel sphere on a glass surface colliding with steel boundary walls.  $\phi$  corresponds to the angle which the final velocity vector makes with the initial velocity vector. The coefficient of restitution is calculated as the square root of the ratio of the final to the initial kinetic energy. The data is distributed over a range of  $r$  which becomes smaller for higher  $\phi$ . The large fluctuations are not related to measurement noise, nor can they be accounted for by variations in the initial velocity [see Fig. 5(b)].

The mean value of  $r$  depends on  $\phi$  and is lower for higher  $\phi$  [indicated by the dashed line in Fig. 5(a)]. The mean value of  $r$  during a wall collision averaged over all  $\phi$  was  $0.5 \pm 0.02$ . In contrast the average loss of energy during a particle-particle collision was lower and the mean  $r$  was found to be 0.65 by averaging over 20 collisions. In comparison, the coefficient of restitution of the steel sphere bouncing off a steel block after being dropped is 0.93. The larger losses in kinetic energy occur mostly because the par-

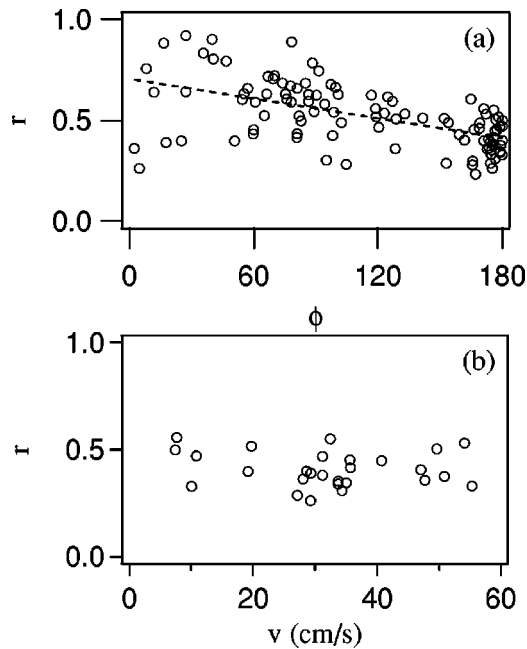


FIG. 5. (a) Effective coefficient of restitution  $r$  versus scattering angle  $\phi$  for a rolling particle colliding off the side walls. The dashed line is a least squares fit to the data. (b) The plot of  $r$  versus initial velocity  $v$  for  $170 \leq \phi \leq 180$  fluctuates significantly.

ticles slide as their angular velocity changes to match their new translational velocity. The change in angular velocity was observed to occur within a centimeter even at the highest velocities observed. It may be possible to approximately model the complications due to rolling by simply assuming a lower value of  $r$ . However, an event-driven simulation using only a loss of kinetic energy in the normal direction does not produce non-Gaussian distributions in  $v_x$ , but yields asymmetric distributions for  $v_y$  [13]. The subtle effects introduced

by rolling may help us understand the effect of higher dissipation on velocity distributions.

Limited experiments were also performed with brass spheres. The distributions obtained were identical to those corresponding to steel spheres under the same conditions. Thus, the velocity distributions obtained are not very sensitive to the details of the surface properties of the spheres.

The distribution of the speed of the particles is a combination of the non-Gaussian or approximately Gaussian velocity distributions of different widths (such as in Figs. 2 and 4) and deviates from the Maxwell-Boltzmann form. Subtle effects on the velocity distributions such as the scaling of the temperature (the second moment of the distributions) in the near elastic limit has been studied theoretically by Kumaran [14], Grossman *et al.* [15], and experimentally by Warr and Huntley [11]. However, the deviations observed in our experiments are stronger as the loss of energy during a collision is significant compared to the energy of the particle. Therefore scaling around the Maxwell-Boltzmann distributions as discussed in Refs. [11,14,15] for  $r \lesssim 1$  cannot be applied to our data.

In conclusion, our experiments on excited dissipative granular matter rolling and bouncing inside a rectangular box have yielded velocity distributions that are strongly non-Gaussian in the absence of significant clustering and density correlations. Our data suggests that caution has to be used in assuming Gaussian velocity distribution and Maxwell-Boltzmann distributions even for rapid granular flows where position correlations are negligible.

We thank J. Tobochnik and H. Gould for many useful discussions, and J. Norton for technical support. This work was supported by the donors of the Petroleum Research Fund, and Grant No. DMR-9983659 from the National Science Foundation. A. K. thanks the Alfred P. Sloan Foundation for its support.

[1] M. A. Hopkins and M. Y. Louge, *Phys. Fluids A* **3**, 47 (1991).  
 [2] I. Goldhirsch and G. Zanetti, *Phys. Rev. Lett.* **70**, 1619 (1993).  
 [3] Y. Du, H. Li, and L. P. Kadanoff, *Phys. Rev. Lett.* **74**, 1268 (1995).  
 [4] A. Kudrolli, M. Wolpert, and J. P. Gollub, *Phys. Rev. Lett.* **78**, 1383 (1997).  
 [5] J. Olafsen and J. Urbach, *Phys. Rev. Lett.* **81**, 4369 (1998).  
 [6] For a review, see C. S. Campbell, *Annu. Rev. Fluid Mech.* **22**, 57 (1990).  
 [7] A. Puglisi *et al.* *Phys. Rev. E* **59**, 5582 (1999).  
 [8] J. S. Olafsen and J. S. Urbach, *Phys. Rev. E* **60**, R2468 (1999).

[9] S. Luding, O. Strauss, and S. McNamara, e-print cond-mat/9910085.  
 [10] L. Kondic, *Phys. Rev. E* **60**, 751 (1999).  
 [11] S. Warr and J. M. Huntley, *Phys. Rev. E* **52**, 5596 (1995).  
 [12] W. Losert, D. Copper, J. Delour, A. Kudrolli, and J. P. Gollub, *Chaos* **9**, 682 (1999).  
 [13] J. Tobochnik (private communications).  
 [14] V. Kumaran, *Phys. Rev. E* **57**, 5660 (1998); **59**, 4188 (1999).  
 [15] E. L. Grossman, T. Zhou, and E. Ben-Naim, *Phys. Rev. E* **55**, 4200 (1997).